

Pulse Delay Via Tunable White Light Cavities Using Fiber-Optic Resonators

Honam Yum, Xue Liu, *Member*, Young Joon Jang, May Eunyeon Kim, and Selim M. Shahriar, *Member, IEEE, Fellow, OSA*

Abstract—Previously, we proposed a data buffering system that makes use of a pair of white light cavities. For application to telecommunication systems, it would be convenient to realize such a device using fiber-optic resonators. In this paper, we present the design of such a system, where the white light cavity effect is produced by using stimulated Brillouin scattering. The system consists of a pair of fiber-optic white light cavities placed in series. As in the original proposal, the delay time can be controlled independently of the bandwidth of the data pulses. Furthermore, we show how the bandwidth of the system can be made as large as several times the Brillouin frequency shift. We also show that the net delay achievable in such a buffer can be significantly larger than what can be achieved using a conventional recirculating loop buffer.

Index Terms—Cavity resonators, optical buffering, optical fiber communication, telecommunication buffers.

I. INTRODUCTION

LOW LIGHT in optical fibers has been of interest due to its applicability to current optical devices for fiber-optic communication such as optical buffers, optical delay lines, and fast memory access [1]–[5]. However, the amount of delay achieved is typically too small to be of interest for most applications. Recently, we have shown that this limitation can be overcome by using fast light, in a manner that is rather counterintuitive [6]. Briefly, this approach makes use of so-called white light cavities (WLCs). A WLC is a cavity containing a fast-light medium, tuned so that negative dispersion causes the wavelength to become independent of frequency over a certain spectral range. As such, it resonates over a broader spectral range compared to an empty cavity of equal length and finesse, without a reduction in the cavity build-up factor [7]. The buffer system is

composed of two WLCs as well as an intervening zone of dispersion-free propagation. When the fast-light medium is deactivated, the WLC acts as a narrowband cavity, which reflects a high-bandwidth pulse stream. However, when the fast-light medium is activated, the data stream passes through the WLC. Using these properties, the data stream can be trapped between the two WLCs for a duration that is limited only by the residual transmission through the cavity in the narrowband mode and the length of the intervening zone. As shown in [6], such a buffer can slow down a data pulse for a duration that is several thousand times longer than the pulse with virtually no distortion. However, for many reasons, a buffer of this type based on free-space components is likely to be impractical, especially for telecommunication. In this paper, we show how to realize such a buffer using WLCs based on fiber resonators, with an optical fiber forming the intervening path.

The buffer presented in this paper has some formal similarity to the dark-state-based scheme employing a pair of microring cavities [8]–[11]. However, the fundamental physical process is quite different, since the concept presented here makes use of anomalous dispersion. We also note that our buffer is similar in configuration to the feedback buffer employing a recirculation loop [12]–[15]. The key difference between our scheme and the feedback buffer is that once the data are in the loop, it is almost completely isolated. During each circulation through the loop, the attenuation is due to a vanishingly small coupling to the WLC and the residual transmission loss inherent to the fiber. As such, there is no need for an amplifier in the loop. A single-stage amplification upon release from the buffer is sufficient to restore the signal level to the input value. Elimination of an intraloop amplifier entails absence of noise due to amplified spontaneous emission, so that for a given level of signal-to-noise ratio (SNR), a much larger number of loop circulations can be allowed. Furthermore, absence of intraloop amplification reduces the energy cost of the buffer.

II. FIBER-BASED FAST-LIGHT DATA BUFFER

Before proceeding with the analysis of a fiber-based fast-light buffer, it is instructive to consider first the basic building block: a fiber resonator coupled to an optical fiber, as illustrated in Fig. 1(a). The model presented here is based on the general configuration of a ring resonator coupled to a waveguide [16]–[20]. We assume that the 2×2 coupler is internally lossless. Thus, the complex amplitudes a_i and b_i are related simply by the intensity coupling coefficient k :

$$\begin{bmatrix} b_1 \\ b_2 \end{bmatrix} = \begin{bmatrix} \sqrt{1-k} & j\sqrt{k} \\ j\sqrt{k} & \sqrt{1-k} \end{bmatrix} \begin{bmatrix} a_1 \\ a_2 \end{bmatrix}. \quad (1)$$

Manuscript received January 12, 2011; revised June 25, 2011; accepted July 05, 2011. Date of publication July 14, 2011; date of current version August 24, 2011. This work was supported in part by DARPA Grant FA9550-07-C-0030, AFOSR Grants FA9550-06-1-0466 and FA9550-10-1-0228, NSF IGERT Grant DGE-0801685, and NASA Grant NNX09AU90A.

H. Yum was with the Department of Electrical Engineering and Computer Science, Northwestern University, Evanston, IL 60208 USA and the Department of Electrical Engineering, Texas A&M University, College station, TX 77843 USA. He is now with the Research Laboratory of Electronics, Massachusetts Institute of Technology, Cambridge, MA 02139 USA (e-mail: hn_yum@mit.edu).

Y. J. Jang and X. Liu are with the Department of Electrical Engineering and Computer Science, Northwestern University, Evanston, IL 60208 USA (e-mail: y-jang@northwestern.edu; xueliu2012@u.northwestern.edu).

M. E. Kim is with the Department of Physics, Northwestern University, Evanston, IL 60208 USA (e-mail: mekim@u.northwestern.edu).

S. M. Shahriar is with the Department of Electrical Engineering and Computer Science and the Department of Physics, Northwestern University, Evanston, IL 60208 USA (e-mail: shahriar@northwestern.edu).

Color versions of one or more of the figures in this paper are available online at <http://ieeexplore.ieee.org>.

Digital Object Identifier 10.1109/JLT.2011.2162090

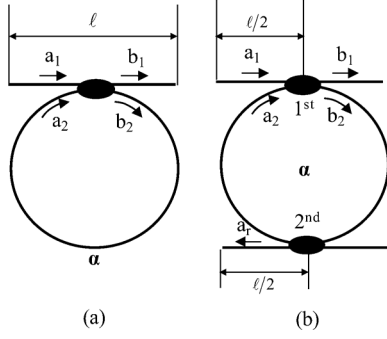


Fig. 1. Schematics of (a) fiber ring resonator and (b) ring resonator coupled to a single-mode fiber.

Next, we express the transmission within the ring resonator as $a_2 = \alpha e^{j\theta} b_2$ in terms of the transmission factor α through the fiber loop and the round trip phase shift θ , which can be expressed as $-\omega n(\omega)L/c$, where L is the circumference of the ring resonator and $n(\omega)$ is the refractive index of the fiber. Using (1), we then get

$$\frac{b_1}{a_1} = \frac{\sqrt{1-k} - \alpha e^{j\theta}}{1 - \alpha\sqrt{1-k}e^{j\theta}} \quad (2)$$

$$\frac{a_2}{a_1} = \frac{j\alpha e^{j\theta} \sqrt{k}}{1 - \alpha e^{j\theta} \sqrt{1-k}}. \quad (3)$$

Fig. 1(b) displays a fiber resonator coupled to a single-mode fiber through the second coupler. It will be a building block for our proposed fiber-based data buffering system. The fiber-coupled resonator can be treated effectively as an uncoupled resonator with additional loss. Therefore, the fields a_i, b_i ($i = 1, 2$) are related by the same matrix as presented in (1), provided that k is replaced by k_1 to represent the coupling coefficient for the first coupler, and α is replaced by $\alpha\sqrt{1-k_2}$, where k_2 is the coupling coefficient of the second coupler. We thus get

$$\frac{b_1}{a_1} = \frac{\sqrt{1-k_1} - \alpha\sqrt{1-k_2}e^{j\theta}}{1 - \alpha\sqrt{1-k_1}\sqrt{1-k_2}e^{j\theta}} \quad (4)$$

$$\frac{a_2}{a_1} = \frac{j\alpha\sqrt{k_1}\sqrt{1-k_2}e^{j\theta}}{1 - \alpha\sqrt{1-k_1}\sqrt{1-k_2}e^{j\theta}}. \quad (5)$$

In addition, the following relations hold:

$$a_2 = \alpha\sqrt{1-k_2}e^{j\theta} b_2 \quad (6a)$$

$$a_r = j\sqrt{\alpha}\sqrt{k_2}e^{\frac{\theta}{2}} b_2. \quad (6b)$$

Combining (5) and (6), we get

$$\frac{a_r}{a_1} = \frac{-\sqrt{\alpha}\sqrt{k_1}\sqrt{k_2}e^{j\frac{\theta}{2}}}{1 - \alpha\sqrt{1-k_1}\sqrt{1-k_2}e^{j\theta}}. \quad (7)$$

In order to take into account dispersion in the fiber loop (induced by stimulated Brillouin scattering, for example), we express $n(\omega)$ in terms of a Taylor expansion about ω_0 :

$$\begin{aligned} n(\omega) &= n_0 + (\omega - \omega_0)n_1 + (\omega - \omega_0)^3 n_3 \\ n_1 &= dn/d\omega|_{\omega=\omega_0} \\ n_3 &= (1/6)dn^3/d\omega^3|_{\omega=\omega_0} \end{aligned}$$

where n_0 is the mean index of the fiber.

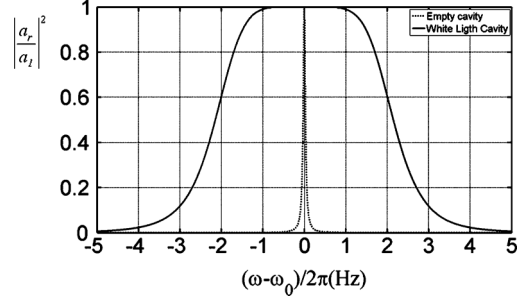


Fig. 2. $|a_r/a_1|^2$ for the fiber-coupled resonator presented in Fig. 1(b). The dashed line is for the case where the resonator is assumed to be nondispersive, while the solid line is for the case where it is anomalously dispersive ($n_1 = -1.192 \times 10^{-15}$ and $n_3 = 9.425 \times 10^{-32}$).

Fig. 2 displays the numerical simulations for $|a_r/a_1|^2$ of an ideal fiber-coupled resonator with no dispersion (dashed line) and with strong negative dispersion (solid line, $n_1 < 0, n_3 \neq 0$). Of course, all fibers have some degree of dispersion. However, dispersion in a typical single-mode fiber is negligible compared to that induced by Brillouin pumps in our system, thus justifying our assumption of $n_1 = 0, n_3 = 0$ for the ideal resonator. For simplicity, we assume unit input intensity $|a_1| = 1$ and no internal loss ($\alpha = 1$). We choose n_1 to fulfill the ideal WLC condition [7]. For the configuration presented in Fig. 1(b), the length of the dispersive medium is assumed to be equal to that of the ring resonator. In that case, the ideal WLC condition requires $n_g = 0$, where n_g is the group index of the dispersive fiber [7]. For nonvanishing n_3 , the WLC linewidth becomes finite. We have chosen $k_1 = k_2 = 0.01, n_0 = 1.45, L = 10.6897$ m, and $\omega_0 = 1.2161 \times 10^{15}$ rad/s, corresponding to a free-space wavelength of 1550 nm, $n_1 = -1.192 \times 10^{-15}$, and $n_3 = 9.425 \times 10^{-32}$.

Here, the value of n_1 is dictated by the WLC condition ($n_g = 0$), the value of n_0 , and the value of ω_0 ($n_1 = n_0/\omega_0$). The value of n_3 was determined by considering a dual Lorentzian gain peaks of the type reported in [21]. In this case, the Brillouin gain bandwidth for each peak was $\Delta\nu_B \approx 2\pi \times 25 \times 10^6$ rad/s, and the separation between the gain peaks is $\delta \approx 1.54\Delta\nu_B$. If we treat the effective gain dip between the two peaks as Lorentzian, then the model shown in [7] yields a value of $n_3 = -n_1/\delta^2 = 8.15 \times 10^{-32}$. A more accurate model, where the index is written as the sum of two Lorentzian gain peaks separated by δ , and the peak amplitudes are adjusted to produce the WLC value of n_1 , yields a value of $n_3 \approx 9.425 \times 10^{-32}$, used in producing Fig. 2. Note that the value of n_3 given by the more accurate model is very close to that given by the simpler model. Thus, it is possible to estimate the linewidth [full-width at half-maximum (FWHM)] of the WLC using the simple relation given in [7]: $\Delta\nu_{WLC} \approx (\Delta\nu_{EC}\delta^2)^{1/3}$, where $\Delta\nu_{EC}$ is the linewidth of the empty cavity. For the parameters used in Fig. 2, we have $\Delta\nu_{EC} \approx 2\pi \times 6.19 \times 10^4$ rad/s, so that we get $\Delta\nu_{WLC} \approx 2\pi \times 4.51 \times 10^6$ rad/s. The value of $\Delta\nu_{WLC}$ as measured from Fig. 2 is $\sim \Delta\nu_{WLC} \approx 2\pi \times 4.3 \times 10^6$ rad/s. Thus, the relation that $\Delta\nu_{WLC} \approx (\Delta\nu_{EC}\delta^2)^{1/3}$ is a reasonable estimate for the linewidth of the WLC as a function of the separation between two Lorentzian gain peaks.

It is instructive here to discuss the values of the experimental parameters necessary to produce the WLC illustrated in Fig. 2. Specifically, we consider bifrequency Brillouin pumps with a frequency separation $S = 2 \times \text{FSR}$, where FSR is the free spectral range of the cavity. Using the data presented in [21], we find the Brillouin coefficient to be $g_0 = 1.01885 \times 10^{-11}$ m/W. By considering the same cavity parameters as used in Fig. 2, and assuming the pumps to be resonant in the cavity, we find the input power needed for Brillouin pump to be ~ 0.33 W.

As can be seen from Fig. 2, the linewidth of WLC is expanded, compared to the ordinary ring resonator associated with $n(\omega) = n_0$. It should be noted that this broadening occurs without a reduction in the cavity build-up factor [7]. If the WLC linewidth is broad enough for the pulse spectrum to be under the resonant spectral region of WLC, then the input signal will transmit without loss or distortion.

Next, we consider the propagation of a pulse through such a fiber-coupled resonator. Equation (7) represents the transfer function between the input and the output. The transfer function is denoted as H_0 for the resonator without dispersion ($n(\omega) = n_0$) and as H_{WLC} under the WLC condition ($n(\omega) = n_0 + (\omega - \omega_0)n_1 + (\omega - \omega_0)^3 n_3$). To find the group velocity associated with the system, it is important to express the group index in terms of $\angle H_{0/\text{WLC}}$, the phase shift induced during propagation through the resonator. The phase contribution resulting from the propagation through the whole system (fiber plus cavity) can be expressed as $(\omega n_{\text{eff}}\ell)/c = (n_0\omega\ell)/c - \angle H_{0/\text{WLC}}$, where we define n_{eff} for the effective refractive index provided by the resonator. By the definition of the group index, obviously $n_{g(\text{resonator})} = n_{\text{eff}} + \omega(dn_{\text{eff}}/d\omega)$, where $n_{g(\text{resonator})}$ is the group index of the whole system (and not the group index of the medium). Thus, $n_{g(\text{resonator})}$, evaluated at $\omega = \omega_0$, a resonance frequency of the cavity centered between the two Brillouin gain peaks, is given by [18]

$$n_{g(\text{resonator})} = n_0 - \frac{c}{\ell} \frac{d\angle H_{0/\text{WLC}}}{d\omega}. \quad (8)$$

Note that the pulse distortion would be characterized [6] by $\Delta T \approx -(d^2\angle H_{0/\text{WLC}}/d\omega^2)\Delta\omega$.

It is instructive to compare $\angle H_{0/\text{WLC}}$ to the phase of b_1/a_1 in (4), denoted as $\angle H_{a_1,b_1}$ in Fig. 3(a). Fig. 3(b) graphically shows the output pulses resulting from propagation through the system, in the presence of the cavities associated with H_0 (dashed) and H_{WLC} (circles) as well as the pulse after propagating a distance ℓ through a fiber only without dispersion (solid). For illustration, we used the cavity parameters in Fig. 2 and chose the input pulse to be of the form $S_{\text{in}}(t) = \exp(-t^2/t_0^2) \exp[j(\omega_0 + \xi)t]$. Here, t_0 is chosen so that $\Delta\nu_{\text{pulse}} = 10\Delta\nu_{\text{cavity}}$, where $\Delta\nu_{\text{pulse}} = 1/t_0$ and $\Delta\nu_{\text{cavity}}$ is the FWHM of the ordinary resonator. Fourier transform of $S_{\text{in}}(t)$ leads us to $\tilde{S}_{\text{in}}(\omega) = t_0/\sqrt{2} \exp[-\{(\omega - \omega_0 - \xi)t_0\}^2/4]$. Applying the convolution theorem, we obtain the amplitude of the output pulse as

$$S_{\text{out}}(t) = 1/\sqrt{2} \int_{-\infty}^{\infty} S(\omega) \times \exp(-jk_0\ell) H_{0/\text{WLC}}(\omega) \exp(j\omega t) d\omega$$

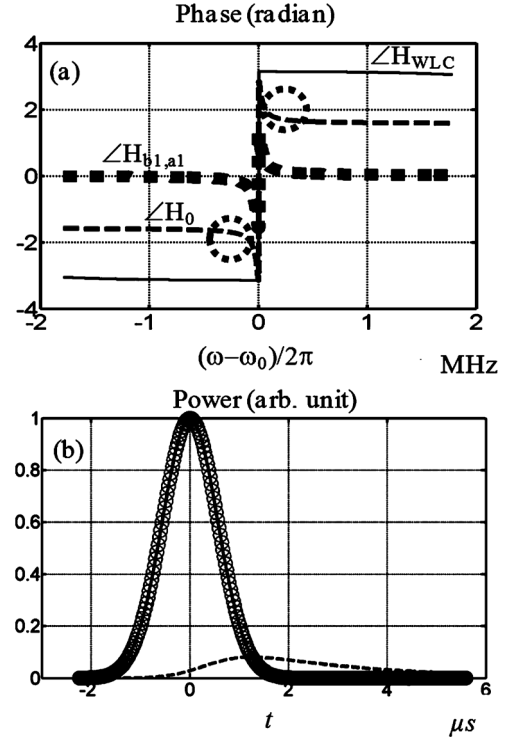


Fig. 3. (a) Phases associated with the transfer functions of the resonator displayed in Fig. 1(b). $\angle H_{b_1,a_1} = \arg(b_1/a_1)$, $\angle H_0 = \arg(a_r/a_1)$ in the absence of WLC effect, and $\angle H_{\text{WLC}} = \arg(a_r/a_1)$ for WLC, with $n_1 = -1.192 \times 10^{-15}$ and $n_3 = 9.425 \times 10^{-32}$. (b) Reference pulse after propagating in a fiber of length ℓ (solid line) and the outputs associated with H_0 (dashed line) and H_{WLC} (circles). The output in the presence of the WLC effect is essentially overlapped with the reference.

where $k_0 = n_0\omega\ell/c$. We simply set $H_{0/\text{WLC}} = 1$ when the field propagates in the fiber only.

Note that there is a discontinuity accompanied by a phase leap at $\omega = \omega_0$ as illustrated in Fig. 3(a). Of course, such a discontinuity disappears when the sources of all losses as well as the finite bandwidth of a real signal are taken into account. However, under the assumptions used here, this result can be explained as follows, in analogy with the critically coupled microresonator presented in [17], for example. Specifically, a critically coupled resonator shows a π -phase leap on resonance. For the resonator considered here, we have used $\alpha = 1$, $k_1 = k_2 = 0.01$, so that $\alpha\sqrt{1-k_2} = \sqrt{1-k_1}$. This means that the transmission factor between b_2 and $a_2(\alpha\sqrt{1-k_2})$ matches the transmission coefficient of the first coupler ($\sqrt{1-k_1}$), corresponding to critical coupling. Thus, $\angle H_{b_1,a_1}$ shows the π -phase leap at resonance. The second coupler, which is identical to the first one, is also critically coupled. Thus, the π -phase leap occurs twice, resulting in a discontinuity of 2π for $\angle H_{0/\text{WLC}}$.

We explain the output pulses illustrated in Fig. 3(b) with the aid of Fig. 3(a). According to (8), the negative slope of $\angle H_0$ suggests $n_{g(\text{resonator})} > n_0$ inside the dotted circle. By setting $\xi = 0$, we have chosen the input pulse to have the carrier frequency equal to ω_0 . As such, the pulse lies within the slow-light zone. Since $\Delta\nu_{\text{pulse}} = 10\Delta\nu_{\text{cavity}}$, most of the pulse spectrum is under the spectral region of $|H_0| = 0$. As a consequence, the output associated with H_0 is delayed and attenuated, as can be seen in Fig. 3(b). For the case of WLC, we consider $\xi = 1.5/t_0$

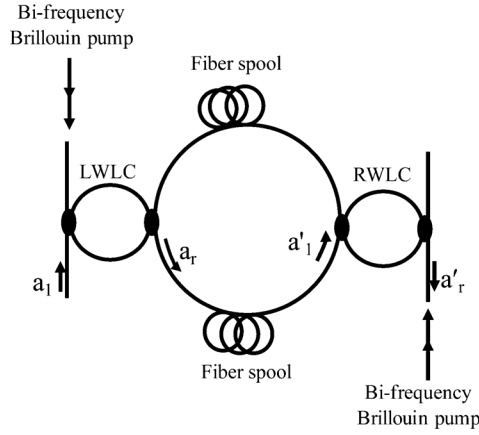


Fig. 4. Schematic illustration of the fiber-based data buffer system, employing bifrequency Brillouin pumps. LWLC: Left white light cavity; RWLC: Right white light cavity.

so as to ensure that the pulse spectrum is mostly outside the region where $\angle H_{\text{WLC}}$ leaps by 2π . Thus, over the spectrum of the pulse, we have $|H_{\text{WLC}}| \simeq 1$, $d\angle H_{\text{WLC}}/d\omega \simeq 0$, and $d^2\angle H_{\text{WLC}}/d\omega^2 \simeq 0$, so that $n_g(\text{WLC}) \simeq n_0$, according to (8). As a result, the output of WLC is not advanced compared to the reference pulse propagating the distance of ℓ through a bare fiber; rather, these outputs are virtually superimposed on each other, as illustrated in Fig. 3(b). This behavior can also be understood physically noting that $n_g = 0$ for the fiber inside the resonator under the ideal WLC condition. Thus, the pulse propagates in the resonator with the speed of $v_g \gg c$, thereby spending very little time inside. Of course, under realistic condition, such a propagation does not violate special relativity or causality [22]. In [23], we describe in detail the exact behavior of a pulse inside a cavity loaded with an anomalously dispersive medium, under a range of conditions, including $n_g = 0$.

In analogy with the previously proposed Fabry–Perot buffer system [6], we now present the design of a fiber-based data buffer, as shown in Fig. 4. We assume that a bifrequency Brillouin pump creates a negative dispersion in a ring resonator to produce the WLC effect, in a manner analogous to the previous WLC demonstration where a bifrequency Raman pump was used to produce dual Raman gain peaks [7], yielding a negative dispersion between the peaks. Here, each Brillouin pump produces a Lorentzian gain peak for the counterpropagating probe. As we discussed earlier, we can reach the WLC condition for a gain separation of $1.54\Delta\nu_B$ ($\Delta\nu_B/2\pi = 25$ MHz in [21]), if we use 0.33 W input power for each Brillouin pump. From the result presented in Fig. 2, we expect $\Delta\nu_{\text{WLC}}/2\pi = 4.51$ MHz. The WLC on the left (LWLC) is connected to the WLC on the right (RWLC) through fiber spools to construct a closed loop where a pulse would be trapped.

For a data pulse and the WLCs, we use the same parameters as considered in Fig. 3. The operating scheme to delay the pulse without distortion is similar to that presented in [6]. When the pulse enters from left, we turn on the bifrequency Brillouin pumps to activate the WLC effect in LWLC. Thus, the pulse transmits through the resonator with no distortion, as shown in Fig. 3(b). Once the pulse has left LWLC, we turn off the WLC

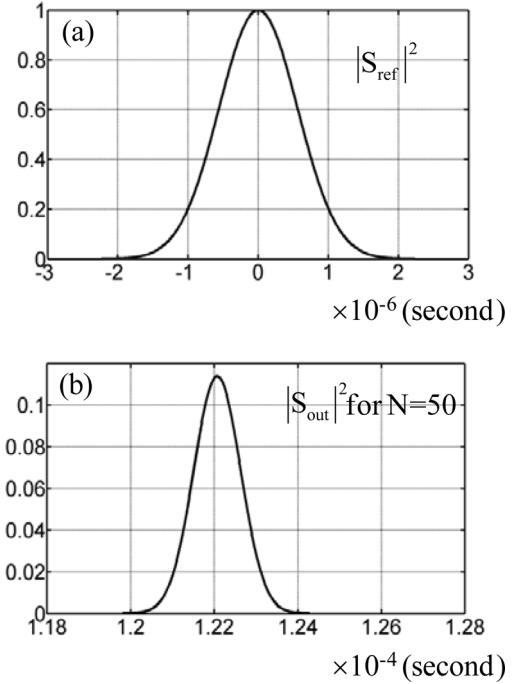


Fig. 5. Output pulses from the fiber-based buffering system. (a) Reference pulse. (b) Pulse after 50 round trips inside the trapping loop.

effect. Now, the pulse is loaded and circulates inside the trapping loop.

To consider power loss during the circulation, it is important to note that the carrier frequency of the pulse is shifted by $\xi = 1.5/t_0$ from the resonant frequency ω_0 of the bare cavity (i.e., without the WLC effect). If it is not shifted, the pulse spectrum would include the transmission window of the bare cavities. In that case, the spectral component within this window would leak out through the bare cavities. With the carrier frequency shifted, LWLC as well as RWLC acts as a simple coupler, with an intensity coupling coefficient of $k_1 = k_2 = 0.01$. On each bounce, the pulse is reflected, with a small transmission loss due to this finite coupling coefficient.

Once we are ready to extract the pulse from the trapping loop, we activate the WLC effect in RWLC. On arriving at RWLC, the pulse passes through it with neither attenuation nor distortion.

To find a full transfer function to describe the data buffer system, we consider the amplitude transfer characteristics $H_{1r} = a_r/a_1$ ($H_{1'r'} = a'_r/a'_1$), where H_{1r} ($H_{1'r'}$) denotes the transfer function of LWLC (RWLC). After N multiple round trips inside the trapping loop, a_r is related to a'_1 by

$$H_{r1'} = \left(\sqrt{1-k_1} \sqrt{1-k_2} \right)^N e^{-jk_0 \frac{2N+1}{2} L_2} 10^{-\frac{\alpha}{20}} \quad (9)$$

where L_2 is the length of the trapping loop and $k_0 = \omega n_0/c$. Here, α represents the total attenuation due to the propagation through the loop. A conventional single-mode fiber for 1550 nm exhibits an attenuation loss of ~ 0.2 dB/km so that $\alpha = 0.2 \times (N + 1/2)L_2$. The time elapsed in the loop represents the system delay: $\tau_d = [n_0(N + 1/2)L_2]/c$. Fig. 5 illustrates the reference pulse propagating a distance ℓ through a fiber, as well as the output from the data buffer for $N = 50$. The reference pulse can be written as

$S_{\text{ref}}(t) = 1/\sqrt{2} \int_{-\infty}^{\infty} \exp(-jk_0\ell) S(\omega) \exp(j\omega t) d\omega$. Using H_{1r} and $H_{1'r'}$ together with (9), the output of the data buffer can be written as

$$S_{\text{out}}(t) = 1/\sqrt{2} \int_{-\infty}^{\infty} \exp(-jk_0\ell) H_{\text{total}} S \times(\omega) \exp(j\omega t) d\omega \quad (10)$$

where $H_{\text{total}} = H_{1'r'}(\omega)H_{r1'}(\omega)H_{1r}(\omega)$. Fig. 5(a) and (b) shows that for $L_2 = 500$, the output pulse is delayed by 1.22×10^{-4} s compared to the reference. Fig. 5(b) indicates that the pulse delay is accompanied by no serious distortion, but an attenuation of about 9.3 dB (from 1 to 0.115). The attenuation per pass is 0.186 dB, which is the sum of attenuation due to transmission (0.1 dB), plus a loss of 1% (0.043 dB) at each of the two couplers.

III. FAST-LIGHT DATA BUFFER VERSUS CONVENTIONAL FIBER-LOOP DATA BUFFER

The attenuation suffered in the storage loop can be compensated by using an optical amplifier. Such an amplifier could be added to the storage loop. However, since the loss per pass in the loop is very small and an amplifier would have an insertion loss much higher than the single-pass attenuation, a better approach is to use a separate loop for the amplification. This is illustrated schematically in Fig. 6(a). Prior to the buffering process, both WLCs are inactive. The pulse stream to be stored is inserted into the trapping loop by activating WLC_1 and deactivating it after the stream is fully loaded. We assume the perimeter of the trapping loop to be 0.5 km (same as the loop considered in Fig. 5). After 50 passes (with an attenuation of 9.3 dB), WLC_2 is activated and the pulse stream enters the amplifying loop. The amplifier in this loop is gated to provide a net amplification (amplifier gain minus the insertion loss of the amplifier) of 9.3 dB, restoring the original amplitude. We neglect the attenuation in the amplifying loop, which can be much smaller. Once the stream reenters the trapping loop, WLC_2 is deactivated. This process is repeated M times after another 50 passes through the trapping loop.

The number of times the amplification is applied, M , is limited by the fact that the SNR is degraded due to noise added during each pass through the amplification process [13]. The actual reduction in SNR during each pass would depend on the type of amplification employed. The maximum allowable net reduction in SNR would depend on the SNR in the input pulse stream and the fidelity requirement of the system. As an example, we consider a case where M is limited to 100. The net delay achievable is then ~ 12.2 ms and the delay-bandwidth product (DBP) for the input pulse used in Fig. 5 would be 10^4 . Obviously, if much shorter pulses are used (which would require a higher bandwidth WLC), the DBP can be correspondingly larger. For example, for a pulsewidth of 0.122 ns (requiring a WLC linewidth of ~ 30 GHz), DBP would be 10^8 .

It is instructive to compare such a system with a conventional recirculating buffer [12]–[15]. A typical implementation of such a buffer is illustrated in Fig. 6(b). Here, during each pass, there is a loss of 7 dB due to the two couplers and the isolator. The net gain (amplifier gain minus the insertion loss of the amplifier)

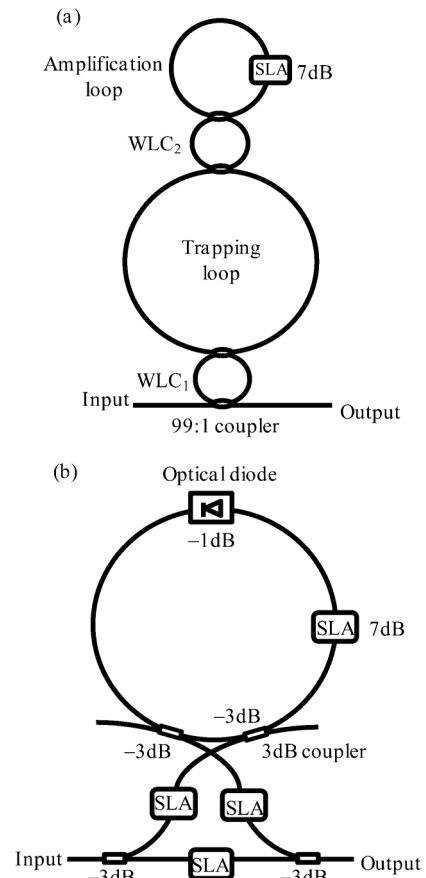


Fig. 6. Schematics illustration of (a) a WLC-based data buffer augmented by amplification and (b) a conventional recirculating data buffer [13]. SLA: Semiconductor laser amplifier; $\text{WLC}_{1,2}$: White light cavity_{1,2}. In (b), the optical diode acts as an isolator.

provided by the amplifier in each pass is thus 7 dB. If all other parameters are comparable to the buffer shown in Fig. 6(a), then the maximum number of amplification for approximately the same reduction in SNR would be about 133 ($=9.3 \times 100/7$). The net delay achievable would be 0.33 ms. Thus, all else being equal, the delay time achievable for the buffer proposed here would achieve a delay of nearly 37 times larger than what can be achieved using a conventional recirculating buffer. This is attributable solely to the fact that the conventional buffer has a large loss (7 dB) per pass, while for the WLC buffer, the inherent loss per pass is much smaller (0.186 dB). The factor by which the WLC delay is larger is essentially a ratio of these two numbers. The relative advantage thus would become better as the loop perimeter becomes smaller and/or couplers with higher efficiency are employed.

IV. ENHANCEMENT OF BANDWIDTH

Next, we discuss a technique for producing a high bandwidth for the data buffer system. From the numerical simulations presented earlier, we find that in general $\Delta\nu_{\text{WLC}}/2$ corresponds to the system bandwidth, where $\Delta\nu_{\text{WLC}}$ is the WLC bandwidth. This is because the pulse spectrum is placed within either one of these two regions, in order to avoid transmission loss at the bare cavity resonance frequency in the trapping loop. The value of $\Delta\nu_{\text{WLC}}$ depends on two important parameters: δ , the gain

separation, and $\Delta\nu_B$, the linewidth of the gain profile. As mentioned earlier, a negative dispersion is created between the two gain profiles. Of course, the slope at the center of the two gains become smaller with decreasing $\Delta\nu_B$ for a particular δ or increasing δ for a particular $\Delta\nu_B$. However, the WLC condition requires a slope that yields a vanishing group index. Thus, for a given value of $\Delta\nu_B$, the value of δ needed for the WLC effect is fixed. This value of δ increases with increasing $\Delta\nu_B$.

For Lorentzian gain peaks, we described previously how the WLC linewidth is closely approximated by the relation $\Delta\nu_{\text{WLC}} \approx (\Delta\nu_{\text{EC}}\delta^2)^{1/3}$, given in [7]. When the gain peaks are Gaussian, it is difficult to develop such a general relation, in part because of the fact that there is no closed form, general solution for the Kramers–Kronig integral for determining the corresponding index. However, to the extent that it is possible to approximate a Gaussian with a Lorentzian, we expect that, at least qualitatively, we would get $\Delta\nu_{\text{WLC}} \approx \zeta(\Delta\nu_{\text{EC}}\delta^2)^{1/3}$, with the value of ζ of the order of unity. Thus, in order to enhance $\Delta\nu_{\text{WLC}}$, it is necessary to increase $\Delta\nu_B$.

Broadening of the Brillouin gain profile can be achieved, for example, by superposing a Gaussian white noise on the dc current of a laser diode [24]–[28] used as a Brillouin pump. In particular, in [28], two Brillouin pumps with equal power, each broadened by white noise, were separated by $2\nu_B$ (where ν_B is the Brillouin frequency shift) to produce a single gain with a bandwidth of $2\nu_B$. Here, we present a scheme to expand the spectral range of a negative dispersion in a similar manner, as illustrated in Fig. 7. We consider first two groups of Brillouin pumps. Each group consists of a pair of pumps with equal power, denoted as pumps A_1 and A_2 (B_1 and B_2). As shown in Fig. 7(a), pumps A_1 and A_2 (B_1 and B_2) are separated by $2\nu_B$ and pumps A_1 and B_1 (A_2 and B_2) by δ . Fig. 7(b) indicates that the spectra of all pumps are broadened so that each pump produces a broadband Brillouin gain with $\Delta\nu_{\text{gain}} \sim \nu_B$.

Note that each pump with frequency ν_p generates an absorption profile at $\nu_p + \nu_B$ with an amplitude equal to that of the gain profile at $\nu_p - \nu_B$. As such, the loss spectra induced by pump A_1 (pump B_1) is compensated by the gain of pump A_2 (pump B_2), since equal-power pumps are used. As displayed in Fig. 7(c), for a single group, it is possible to increase $\Delta\nu_B$ until the tail of the gain profile produced by pump A_1 (pump B_1) meets that of the absorption of pump A_2 (pump B_2). Accordingly, we get $\Delta\nu_B \simeq 2\nu_B$.

In what follows, we assume $\nu' \simeq 2\Delta\nu_B$, where ν' is the width measured along the bottom of the gain. For the two groups of pumps, it is important to consider the overlap of the net loss profile of A_2 with the gain profile of B_1 . Note that, as illustrated in Fig. 7(d), these two profiles meet in the encircled area if $\Delta\nu_B \simeq 2\nu_B$. Such an overlap distorts the net gain profile. In order to avoid it, the parameters under consideration should satisfy the condition that $\delta + \nu'/2 \leq 2\nu_B$.

In principle, N pumps can create a single gain with a maximum bandwidth equal to $N\nu_B$ [28]. In that case, $2N\nu_B$ is the spectral distance between the gain peak of pump A_1 and the absorption dip of pump A_N . To ensure that the tail of the gain profile of pump B_1 does not encounter that of the absorption profile of pump A_N , the condition is $\delta + \nu'/2 \leq 2(N-1)\nu_B$. Fig. 8 displays the gain profiles for a particular condition: $N = 3$,

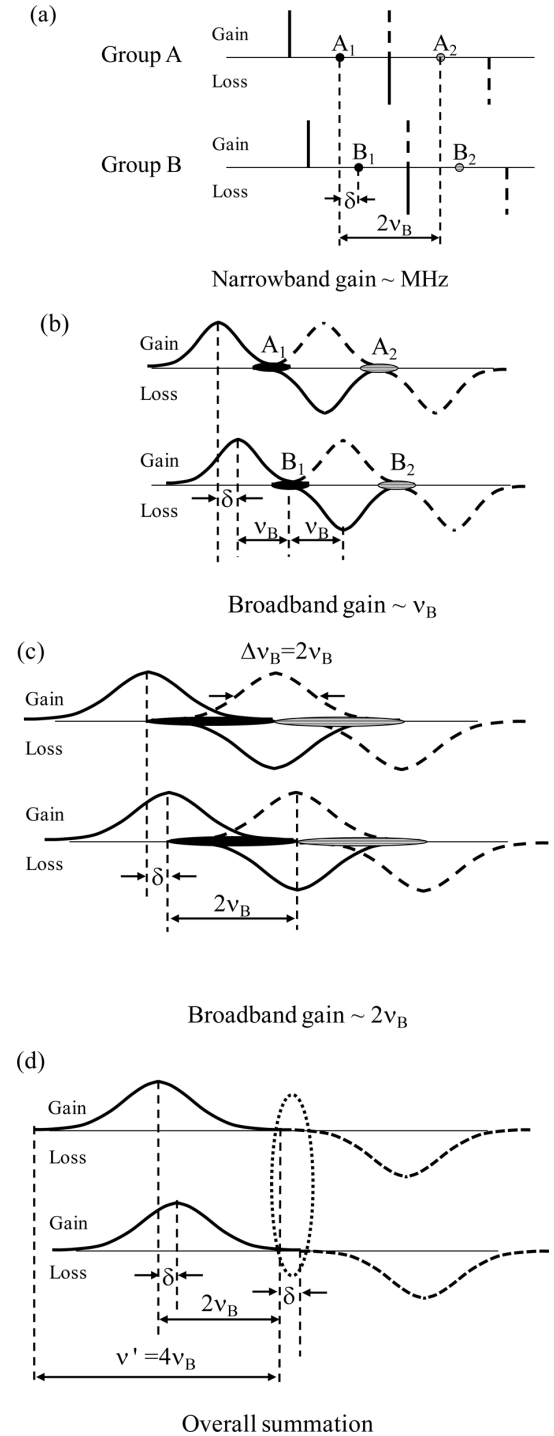


Fig. 7. Illustration of a scheme to increase δ and $\Delta\nu_B$ using broadband Brillouin pumps. (a) In the absence of Gaussian white noise, the pumps produce the narrowband Brillouin gain/loss spectrum. (b) Linewidth of the pumps is broadened by the white noise. The gain bandwidth is expanded to ν_B , and eventually reaches the maximum of $2\nu_B$. (c) In the encircled area, the net gain in group B is overlapped with the net loss in group A. In figures, the gain/loss profiles of A_1 , B_1 and A_2 , B_2 are represented by solid lines and dashed lines, respectively.

$\Delta\nu_B = 2\nu_B$, $\delta = 2\nu_B$, and $\nu' = 4\nu_B$. Fig. 8(a) indicates that the gain of pump A_{N+1} (B_{N+1}) counters the loss due to pump A_N (B_N) ($N = 1, 2$). In Fig. 8(b), the gain profiles of pump A_1 and B_1 remain, and thus the net gain profile is a gain

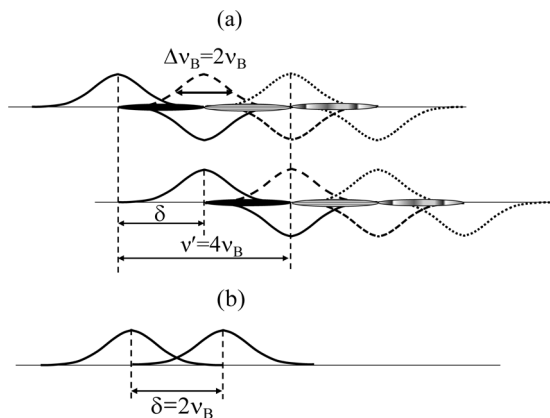


Fig. 8. (a) Each group consists of three broadband pumps. $\delta\nu_B = 2\nu_B$, $\Delta = 2\nu_B$, and $v' = 4\nu_B$. (b) Overall summation. Net gain profile is a gain doublet with $\delta = 2\nu_B$.

doublet with the separation of $\delta = 2\nu_B$. The Brillouin frequency of conventional optical fibers is 8–12 GHz according to [21] and [29]. Thus, for example, with $N = 11$, $\nu_B = 10$ GHz, and $\Delta\nu_B = 10\nu_B$, it is possible to get $\delta = 100$ GHz. Using the approximate expression for the WLC linewidth for a Gaussian gain doublet discussed previously, with α assumed to be close to unity and $\Delta\nu_{EC}/2\pi \approx 100$ MHz, for example, we get $\Delta\nu_{WLC}/2\pi \approx 10$ GHz.

V. CONCLUSION

To summarize, we present the design of a fiber-based fast-light data buffer system, consisting of a pair of WLCs placed in series. The WLC effect is produced by using stimulated Brillouin scattering. The delay time can be controlled independently of the bandwidth of the data pulses, thus circumventing the DBP constraint faced by conventional buffer systems. We also show that the net delay achievable can be significantly larger than what can be achieved with a conventional recirculating loop buffer.

REFERENCES

- [1] Y. Okawachi, M. S. Bigelow, J. E. Sharping, Z. Zhu, A. Schweinsberg, D. J. Gauthier, R. W. Boyd, and A. L. Gaeta, "Tunable all-optical delays via Brillouin slow light in an optical fiber," *Phys. Rev. Lett.*, vol. 94, pp. 153902–, Apr. 2005.
- [2] K. Y. Song, M. G. Herráez, and L. Thévenaz, "Observation of pulse delaying and advancement in optical fibers using stimulated Brillouin scattering," *Opt. Exp.*, vol. 13, no. 1, pp. 82–88, Jan. 2005.
- [3] K. Y. Song, K. S. Abedin, and K. Hotate, "Gain-assisted superluminal propagation in tellurite glass fiber based on stimulated Brillouin scattering," *Opt. Exp.*, vol. 16, no. 1, pp. 225–230, Jan. 2008.
- [4] K. Y. Song, K. S. Abedin, K. Hotate, M. G. Herráez, and L. Thévenaz, "Highly efficient Brillouin slow and fast light using As₂Se₃ chalcogenide fiber," *Opt. Exp.*, vol. 14, no. 13, pp. 5860–5865, Jun. 2006.
- [5] Z. Zhu, D. J. Gauthier, and R. W. Boyd, "Stored light in an optical fiber via stimulated Brillouin scattering," *Science*, vol. 318, no. 5857, pp. 1748–1750, Dec. 2007.
- [6] H. N. Yum, M. E. Kim, Y. J. Jang, and M. S. Shahriar, "Distortion free pulse delay system using a pair of tunable bandwidth white light cavities," *Opt. Exp.*, vol. 19, no. 7, pp. 6705–6713, Mar. 2011.
- [7] G. S. Pati, M. Salit, K. Salit, and M. S. Shahriar, "Demonstration of a tunable-bandwidth white light interferometer using anomalous dispersion in atomic vapor," *Phys. Rev. Lett.*, vol. 99, pp. 133601–, Sep. 2007.
- [8] Q. Xu, S. Sandhu, M. L. Povinelli, J. Shakya, S. Fan, and M. Lipson, "Experimental realization of an on-chip all optical analogue to electromagnetically induced transparency," *Phys. Rev. Lett.*, vol. 96, pp. 123901–, Jul. 2006.

- [9] Q. Xu, P. Dong, and M. Lipson, "Breaking the delay-bandwidth limit in a photonic structure," *Nat. Phys.*, vol. 3, pp. 406–410, Jun. 2007.
- [10] J. Scheuer, A. A. Sukhorukov, and Y. S. Kivshar, "All-optical switching of dark states in nonlinear coupled microring resonators," *Opt. Lett.*, vol. 35, no. 21, pp. 3712–3714, Nov. 2010.
- [11] P. Dong, L. Chen, Q. Xu, and M. Lipson, "On-chip generation of high-intensity short optical pulses using dynamic microcavities," *Opt. Lett.*, vol. 35, no. 15, pp. 2315–2317, Aug. 2009.
- [12] E. F. Burmeister, D. J. Blumenthal, and J. E. Bowers, "A comparison of optical buffering technologies," *Opt. Switch. Netw.*, vol. 5, no. 1, pp. 10–18, Mar. 2008.
- [13] R. Langenhorst, M. Eiselt, W. Pieper, G. Grobkopf, R. Ludwig, L. Kuller, E. Dietrich, and H. G. Weber, "Fiber loop optical buffer," *J. Lightw. Technol.*, vol. 14, no. 3, pp. 324–335, Mar. 1996.
- [14] A. Agrawal, L. Wang, Y. Su, and P. Kumar, "All-optical loadable and erasable storage buffer based on parametric nonlinearity in fiber," *J. Lightw. Technol.*, vol. 23, no. 7, pp. 2229–2238, Jul. 2005.
- [15] K. Hall and K. Rauschenbach, "All-optical buffering of 40-Gb/s data packets," *IEEE Photon. Technol. Lett.*, vol. 10, no. 3, pp. 442–444, Mar. 1998.
- [16] A. Yariv, "Universal relations for coupling of optical power between microresonators and dielectric waveguides," *Electron. Lett.*, vol. 36, no. 4, pp. 321–322, Feb. 2000.
- [17] J. E. Heebner and R. W. Boyd, "'Slow' and 'fast' in resonator-coupler waveguide," *J. Mod. Opt.*, vol. 49, no. 14/15, pp. 2629–2636, 2002.
- [18] J. E. Heebner, R. W. Boyd, and Q. Park, "Slow light, induced dispersion, enhanced nonlinearity, and optical solitons in a resonator-array waveguide," *Phys. Rev. E*, vol. 65, p. 036619, Mar. 2002.
- [19] J. K. S. Poon, J. Scheuer, S. Mookherjee, G. T. Paloczi, Y. Huang, and A. Yariv, "Matrix analysis of microring coupled-resonator optical waveguides," *Opt. Exp.*, vol. 12, no. 1, pp. 90–103, Jan. 2004.
- [20] J. E. Heebner, R. W. Boyd, and Q. Park, "SCISSOR solitons and other novel propagation effects in microresonator-modified waveguides," *J. Opt. Soc. Amer. B*, vol. 19, no. 4, pp. 722–731, Apr. 2002.
- [21] A. Loayssa, R. Hernández, D. Benito, and S. Galech, "Characterization of stimulated Brillouin scattering spectra by use of optical single-sideband modulation," *Opt. Lett.*, vol. 29, no. 6, pp. 638–640, Mar. 2004.
- [22] L. J. Wang, A. Kuzmich, and A. Dogariu, "Gain-assisted superluminal light propagation," *Nature*, vol. 406, pp. 277–279, Jul. 2000.
- [23] H. N. Yum, Y. J. Jang, and M. S. Shahriar, "Pulse propagation through a dispersive intracavity medium," [Online]. Available: //arxiv.org/abs/1012.4483
- [24] A. Zadok, A. Eyal, and M. Tur, "Extended delay of broadband signals in stimulated Brillouin scattering slow light using synthesized pump chirp," *Opt. Exp.*, vol. 14, no. 19, pp. 8498–8505, Sep. 2006.
- [25] S. H. Chin, M. G. Herráez, and L. Thévenaz, "Zero-gain slow & fast light propagation in an optical fiber," *Opt. Exp.*, vol. 22, no. 22, pp. 10684–10692, Oct. 2006.
- [26] R. Pant, M. D. Stenner, M. A. Neifeld, and D. J. Gauthier, "Optimal pump profile designs for broadband SBS slow-light systems," *Opt. Exp.*, vol. 16, no. 4, pp. 2764–2777, Feb. 2008.
- [27] A. A. Juárez, R. Vilaseca, Z. Zhu, and D. J. Gauthier, "Room-temperature spectral hole burning in an engineered inhomogeneously broadened resonance," *Opt. Lett.*, vol. 33, no. 20, pp. 2374–2376, Oct. 2008.
- [28] K. Y. Song and K. Hotate, "25 GHz bandwidth Brillouin slow light in optical fibers," *Opt. Lett.*, vol. 32, no. 3, pp. 217–219, Feb. 2007.
- [29] K. S. Abedin, "Stimulated Brillouin scattering in single-mode tellurite glass fiber," *Opt. Exp.*, vol. 14, no. 24, pp. 11766–11772, Nov. 2006.

Honam Yum received the B.S. degree in ceramic engineering from Yonsei University, Seoul, Korea. He received the M.S. and Ph.D. degrees in electrical and computer engineering, from Texas A&M University, College Station, in 2004 and 2009, respectively.

From 2004 to 2006, he was with a Liquid Crystal Display division of Samsung Electronics, Seoul, Korea. He was a Postdoctoral Fellow at Northwestern University, Evanston, IL. His research during M.S. degree was focused on angular multiplexed holographic gratings to combine multiple coherent light sources. During Ph.D. and the postdoctoral appointment, he focused on superluminal pulse propagation in a photorefractive crystal, fast-light medium in an optical resonator and its applications to hypersensitive optical sensing, and optical buffers with high delay-bandwidth product. He is currently a Postdoctoral Associate at the Massachusetts Institute of Technology, Cambridge. His current research interests include nitrogen vacancy center in diamond for the applications in quantum information processing.

Xue Liu received the B.S. degree in electronic science and technology from the Harbin Institute of Technology, Harbin, China, in 2005, and the M.S. degree in electro-optics in 2008 from University of Dayton, Dayton, OH. He is currently working toward the Ph.D. degree in electrical engineering and computer science at Northwestern University, Evanston, IL.

His research interests include polarimetric imaging, optical coherence tomography, and optical data buffering.

Mr. Liu is a member of the Optical Society of America.

Young Joon Jang received the B.S. degree in electrical engineering from Northwestern University, Evanston, IL, in 2010, where he is currently working toward the M.S. degree in electrical engineering.

His research interests include fiber-optic communication and data buffer system.

May Eunyeon Kim received the B.A. degree from Wellesley College, Wellesley, MA, in 2002, and the M.S. degree in physics from Michigan Technological University, Houghton, MI, in 2007. She is currently working toward the Ph.D. degree in physics at Northwestern University, Evanston, IL.

Ms. Kim is a Fellow of National Science Foundation's Integrative Graduate Education and Research Traineeship Program.

Selim M. Shahriar (M'02) received the B.S., M.S., and Ph.D. degrees in electrical engineering from the Massachusetts Institute of Technology, Cambridge, MA, in 1986, 1989, and 1991, respectively.

From 1991 to 2001, he was at the Research Laboratory of Electronics at Massachusetts Institute of Technology, serving as a Postdoctoral Associate from 1991 to 1992, as a Research Scientist from 1992 to 1999, and as a Principal Research Scientist from 1999 to 2001. He joined Northwestern University, Evanston, IL, in 2001 as an Associate Professor in the Department of Electrical Engineering and Computer Science. Since 2008, he has been a Professor and the Chair of the Division of Solid State and Photonics in the Department of Electrical Engineering and Computer Science, and a Professor in the Department of Physics and Astronomy at Northwestern University. He is a member of the Center for Photonic Communication and Computing, a member of the Center for Interdisciplinary Exploration and Research Activities at Northwestern University, and a member of the LIGO Scientific Collaboration. He is the author or coauthor of more than 100 journal papers and 190 conference papers. His research interests include applications of slow and fast light, quantum information processing, holographic and polarimetric image processing, atomic interferometry, and precision metrology.

Dr. Shahriar is a Fellow of the International Society for Optical Engineers and the Optical Society of America.